

Changing thin-film growth by modulating the incident flux

Nicolas Combe and Pablo Jensen*

Département de Physique des Matériaux, Université Claude Bernard Lyon-1, 69622 Villeurbanne Cédex, France

(Received 12 September 1997; revised manuscript received 1 December 1997)

Thin films are usually obtained by depositing atoms with a continuous flux. We show that using a chopped flux leads to different morphologies or growth regimes. For example, growth cannot be simply understood by replacing the chopped flux by its average (or instantaneous) value and using the usual growth theories: different regimes appear, and in one of them the diffusion constant has no effect on the saturation island density, contrary to what is observed in all theories with continuous fluxes. We present a simple scaling analysis to predict how the island densities change as a function of the frequency of the chopped flux in several growth regimes: *irreversible* aggregation with mobile islands, *reversible* aggregation (critical island size greater than 1). These predictions are confirmed by computer simulations. The model is useful to study growth over a larger range of growth conditions, especially for the growth of thin films prepared by *pulsed* sources. [S0163-1829(98)05524-6]

The technological importance of thin films has given impetus to an intense effort for understanding their growth these last 30 years. One of the main characteristics of growth in usual deposition conditions is that the structure of the deposited films is to a large extent determined by kinetic factors, as opposed to thermodynamic equilibrium. This complicates the analysis of the growth since one cannot simply try to find the state of lowest free energy. Instead, it is necessary to follow in detail how atoms behave after reaching the surface and how they incorporate into the film. A first step in this direction was first accomplished by Zinsmeister¹ using a mean-field approach to establish rate equations of growth. Further help originated from two technological developments: experimentally, scanning tunneling microscopy permits now to check atomic models of growth by giving images of the growing film at the atomic scale²⁻⁴ and theoretically, rapid computer simulations are now feasible to investigate the effects of given atomic processes.^{5,6} While this kinetic control of the film structure complicates its study, the advantage is that one can “play games”⁹ with the different growth parameters (incident flux of particles, diffusion coefficient of an adatom, etc.) in order to obtain different film morphologies. A simple example is given by the quantity of islands grown on a perfect substrate at low enough temperatures: it is known that the number of islands at saturation scales as $(F/D)^{1/3}$ (Refs. 10–12) where F is the incident flux and D the diffusion coefficient. Then, by increasing the flux or decreasing the diffusion constant (by lowering the substrate temperature), one can adjust the saturation number of islands grown on the substrate. In this sense, each kinetic factor is a “handle” on the system, allowing to control the morphology of the films. We introduce here a new kinetic handle, which should enable a larger control over film growth: the *chopping* of the incident flux. We note that this flux modulation is intrinsic to other deposition techniques such as cluster laser vaporization (the laser is pulsed¹³). It is therefore important to understand how growth proceeds in the presence of a modulated flux if one is to be able to interpret experiments performed in these conditions. For example, one may wonder whether the usual growth

theories¹⁰⁻¹² can be used by replacing the continuous flux by the average value of the chopped flux over a cycle. In the following, we will show that this is not the case, and that the growth of the film is profoundly changed by the modulation of the incident flux. We will analyze growth in two different limits: the *irreversible* aggregation limit, including mobile islands, and the case of *reversible* aggregation.

The basic idea is that if instead of using a continuous flux we use a *chopped* flux to grow a film, the number of islands formed on a substrate will depend on the chopping frequency f and on d , the fraction of the period the flux is “on” (see Fig. 1). This dependence is due to the fact that the free particle concentration on the surface does not reach its steady-state concentration instantaneously, but only after a characteristic time which we will call τ_m . Then, if the timescale of the chopping ($1/f$) is much smaller than τ_m , the system only sees the average flux. In the contrary case, everything happens as if the instantaneous flux was used instead. Then, there will be a transition from one behavior to the other at a chopping frequency close to $1/\tau_m$.

The basic model studied in this paper includes the following: (1) *Deposition*. Particles are deposited at randomly chosen positions of the surface at a flux F_i during the “on” fraction of a cycle ($d < 1$). During the rest of the cycle, no

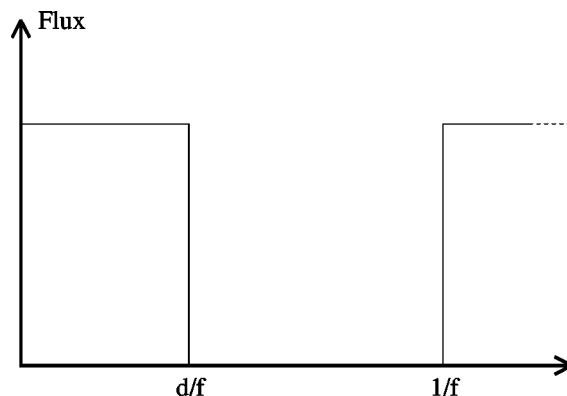


FIG. 1. Illustration of the chopped flux.

particle reaches the surface (see Fig. 1). The average flux reaching the surface is thus $F_{av} = dF_i$. (2) *Diffusion*. Entities can move in a random direction by one diameter, or one lattice spacing, which we will take as our unit length. We denote by τ the characteristic time between diffusion steps. (3) *Aggregation*. If two adatoms come to occupy neighboring sites, they stick to form an island. This is the basic model that we will study in two limiting cases.

First, in the limit of *irreversible* aggregation, we suppose that monomers cannot detach from islands and cannot diffuse on the edges of islands, but *we allow islands to move*: the case of immobile islands has already been studied in a previous paper.¹⁴ More precisely, we only allow islands of size smaller than i_{max} to move, and their diffusion coefficient is inversely proportional to their mass⁶ (i.e., its number of particles) as discussed below. The inclusion of island mobility is motivated by the fact that many researchers have suggested that island diffusion can be an important process in film growth.^{12,15–17} It was therefore important to include this possibility in the model. One could argue that island diffusion occurs via atomic diffusion along the island edge and that moving the islands as a *rigid* entity is not realistic. However, the precise mechanism of island diffusion is not important here, and we only need to know how fast islands can move. The only possible problem is that islands moving by edge diffusion are compact, whereas our islands remain ramified, but this is not important for *small* islands (in the present study the largest clusters allowed to move contain seven sites). Concerning the size dependence of the island diffusion, in the absence of any universal law observed experimentally (the laws vary from $D_N \sim N^{-0.5}$ to $D_N \sim N^{-1.5}$ depending on the precise diffusion mechanisms^{7,8}) we choose a reasonable inverse mass law. Since we only aim at obtaining *scaling* laws, the detailed value of this exponent should not be critical.

The effects of island mobility for irreversible aggregation are studied in next section. Section II deals with the opposite case of *reversible* aggregation where we suppose that every particle can move with a probability which is an exponentially decreasing function of its number of neighbors.¹⁸ This means that islands can break up, which is the most common situation experimentally, as soon as the growth temperature is not too low, and that diffusion on the island edge is allowed. Thus, including both *irreversible* and *reversible* aggregation allows to have a broad view on many different experimental situations.

I. IRREVERSIBLE AGGREGATION

We start with the simplest case of irreversible aggregation and *immobile* islands ($i_{max} = 1$). This situation has been analyzed previously¹⁴ and we only summarize here the main results. The analysis is simple because the only “active” particles for island nucleation are the monomers and therefore the only relevant time scale is the time during which the monomers can nucleate a new island, which is the same as the time between their deposition and their incorporation into a pre-existing island.¹⁹ Since, in the absence of evaporation, the monomers disappear mainly by diffusing randomly until they aggregate with an island,¹⁰ their mean lifetime on the surface is given by $\tau_m \sim l^2/D$ where $2l$ is the mean distance

between islands and D the diffusion constant of the monomers. We obtain $\tau_m \sim 1/(DN)$ where N is the island concentration. We can predict three regimes of behavior, depending on the relative magnitude of τ_m , d/f and $1/f$.

For low chopping frequencies ($\tau_m \ll d/f$), the monomer concentration reaches its steady-state concentration $\rho_{ss} = F_i \tau_m$ almost instantaneously in the time scale of a period. After the flux is turned off, the monomer concentration goes back to 0 also almost instantaneously ($\tau_m \ll d/f \ll 1/f$). Then, between two successive “flux on” periods, nothing happens since only the monomers can move, and there is no monomer left. Therefore, growth proceeds as if we had a continuous flux F_i and the island concentration at saturation for low frequencies N_{sat}^{lf} satisfies the well-known result $N_{sat}^{lf} \sim (F_i/D)^\chi$, with $\chi \sim 0.36$ for fractal islands.¹⁰

We then cross to the regime of high frequencies ($\tau_m \gg 1/f$), where many deposition cycles are carried out during the monomer equilibration, and the system only sees the average flux $F_{av} = F_i d$. Then the island concentration at saturation for high frequencies N_{sat}^{hf} satisfies $N_{sat}^{hf} \sim (F_{av}/D)^\chi = d^\chi N_{sat}^{lf} \ll N_{sat}^{lf}$.

In the intermediate case ($d/f \ll \tau_m \ll 1/f$), a more complex analysis must be done and one obtains $N_{sat} \sim (F_i d/f)^{1/2}$.

Computer simulations¹⁴ are in very good agreement with these predictions.

A. Scaling laws ($i_{max} = 2$)

In this section, we will try to make some predictions for the growth in the different regimes in the case $i_{max} = 2$: only monomers and dimers can move. We show that introducing dimer motion changes the exponents in the three regimes evoked above. It is already known that the motion of the dimers changes the scaling laws from the case $i_{max} = 1$ in the case of a continuous flux.^{10,15,17}

Let us call ρ_1 the monomer concentration, ρ_2 the dimer concentration, N the island concentration, D_1 the monomer diffusion coefficient, and D_2 the dimer one. We will assume that D_1 and D_2 have the same order of magnitude but are different. As in the case $i_{max} = 1$ (immobile islands), we call f the frequency of the chopping flux and d the fraction of the cycle the flux is “on.” We have also to introduce $\tau_1 = 1/D_1 N$ the average time the monomers need to aggregate on an island, and $\tau_2 = 1/D_2 N$ the average time the dimers need to disappear from the substrate by dimer-island aggregation. Since $D_1 \approx D_2$, $\tau_1 \approx \tau_2$.

We can now investigate the different regimes of growth depending on the relative magnitude of τ_1 , τ_2 , d/f , $1/f$.

For low frequency chopping ($\tau_1, \tau_2 \ll d/f$), the monomer and dimer concentrations reach their steady value almost instantaneously when the flux is “on” and vanish instantaneously when the flux is “off.” So, as in the case $i_{max} = 1$, the system behaves as if the flux were continuous with a value F_i and the scaling law giving the island concentration at saturation N_{sat} is¹⁰

$$N_{sat} \sim \left(\frac{F_i^2}{D_1 D_2} \right)^{1/5}. \quad (1)$$

This equation is valid only when dimer diffusion is high enough to change island density (see Ref. 10 for a more detailed analysis).

For high frequency chopping ($1/f \ll \tau_1, \tau_2$), as in the case $i_{\max} = 1$ and for the same reasons, the system behaves as if the flux were continuous with the average value: $F_{\text{av}} = F_i d$. And so the scaling law is

$$N_{\text{sat}} \sim \left(\frac{(F_i d)^2}{D_1 D_2} \right)^{1/5}. \quad (2)$$

For intermediate regime ($d/f \ll \tau_1, \tau_2 \ll 1/f$), we have to perform a more careful analysis. For this, the usual mean-field equations are^{1,10,12,20,21}

$$\frac{d\rho_1}{dt} \simeq F(t) - D_1(\rho_1)^2 - D_1\rho_1 N - (D_1 + D_2)\rho_1\rho_2, \quad (3)$$

$$\frac{d\rho_2}{dt} \simeq D_1(\rho_1)^2 - D_2\rho_2 N - (D_1 + D_2)\rho_1\rho_2 - D_2(\rho_2)^2, \quad (4)$$

$$\frac{dN}{dt} \simeq (D_1 + D_2)\rho_1\rho_2 + D_2(\rho_2)^2. \quad (5)$$

In Eq. (3), the first term of the right-hand side denotes the flux of monomers on the surface, the second and third terms represent, respectively, the loss of monomers by monomer-monomer and monomer-island aggregation, the fourth represents the loss of monomers by monomer-dimer aggregation, and take in account motions of monomers and dimers. Equations (4) and (5) have similar terms.

To solve these equations, we make two hypothesis: we assume that $\rho_1 \ll N$ and $\rho_2 \ll \rho_1$. This leads to

$$\frac{d\rho_1}{dt} \simeq F(t) - D_1\rho_1 N, \quad (6)$$

$$\frac{d\rho_2}{dt} \simeq D_1(\rho_1)^2 - D_2\rho_2 N, \quad (7)$$

$$\frac{dN}{dt} \simeq (D_1 + D_2)\rho_1\rho_2. \quad (8)$$

Solving Eqs. (6) and (7) during one period [with the condition $\rho_1(t=0) = \rho_2(t=0) = \rho_1(t=1/f) = \rho_2(t=1/f) = 0$], and calculating the increase $\Delta N_{\text{cycle}} = \int_{\text{cycle}} (D_1 + D_2)\rho_1\rho_2 dt$ of islands during the same time, one finds

$$\Delta N_{\text{cycle}} = (F_i d/f)^3 \frac{1}{N^2} \left[1 + \frac{d}{f\tau_1} + \left(\frac{d}{f\tau_1} \right)^2 \left(1 + \frac{\tau_1}{\tau_2} \right) \right]. \quad (9)$$

And since $d/f \ll \tau_1, \tau_2 \ll 1/f$, we have

$$\Delta N_{\text{cycle}}^3 \approx (F_i d/f)^3. \quad (10)$$

The number of cycles done is a function of the surface coverage θ (the number of occupied sites divided by the total number of sites of the lattice): $n_{\text{cycle}} = \theta f / F_i d$. We stop simulations when the island concentration reaches its maximum:

we have checked that it occurs for $\theta = 0.15$ as for the continuous flux.^{6,20} So we finally obtain the scaling law for the intermediate regime:

$$N_{\text{sat}} \sim \left(\frac{F_i d}{f} \right)^{2/3}. \quad (11)$$

B. Computer simulations

We now perform Monte Carlo simulations to check these calculations. As explained in the introduction, our program includes the following:^{6,14,20} *Deposition*. Monomers are dropped on the lattice at random positions with a flux F_i during the ‘‘on’’ fraction of the cycle. During the rest of the cycle, no monomer reaches the surface. *Diffusion*. Every island (including monomers) of size smaller than i_{\max} can move in a random direction by one lattice site. *Aggregation*. When two islands (or monomers) meet, they stick irreversibly to form a single island.

More precisely, the algorithm is written in the following way. Each loop we increase the time by $dt = 1/D_1(F_i L^2 + N_{\text{Clueff}})$, where N_{Clueff} is the number of mobile species (monomers and islands of size smaller than i_{\max}) at that time, L is the lattice size and $1/D_1$ is the diffusion time of a monomer from a lattice site to a neighbor. Within this loop, we perform only one operation: diffusion or deposition.

(i) The probability of moving a particle is $N_{\text{Clueff}}/(F_i L^2 + N_{\text{Clueff}})$: we randomly choose an island or a monomer among N_{Clueff} and move it by one lattice site according to its mobility. In the absence of any systematic law observed experimentally (see above), we chose a simple law for the mobility of the clusters: diffusion coefficient proportional to the inverse of the mass of the island.

(ii) The probability of deposition is $F_i L^2/(F_i L^2 + N_{\text{Clueff}})$: an empty site of the lattice is chosen at random and we deposit a new particle there. It can easily be checked that these probabilities reproduce the physical definitions of the flux and the diffusion we want to simulate.

We now analyze the dependence of the saturation island concentration on the chopping frequency. Figure 2 shows the results obtained for $i_{\max} = 2$ on a square lattice for different values of d (fraction of the period the flux is ‘‘on’’). We can first note that the three regimes predicted are actually present. Moreover, the dependence on the frequency f in the intermediate regime is in good agreement with the prediction: the solid line is a fit of the ($d = 0.0001$) curve and has a slope 0.70 whereas the prediction is $2/3$. Moreover, we can check that the ratio of island concentration between high and low frequencies regimes agrees with the predicted ratio $d^{2/5}$.

Figure 3 shows the saturation island density as a function of the rescaled flux (F/D) for different values of the frequency. We can check that in the low- and high-frequency regimes, the slopes of the curves are in good agreement with the predicted ones $2/5$. Moreover, for intermediate frequency, we can point out three different parts of the curve: for high and low fluxes, the curves tend asymptotically towards the low- and high-frequency regimes, and for the intermediate one, the system is in fact in the regime $d/f \ll \tau_1, \tau_2 \ll 1/f$, and we can check that the dashed line of slope $2/3$ fits the data quite well (a fit would give a slope of 0.62). Note that here, the change of regime for the intermediate

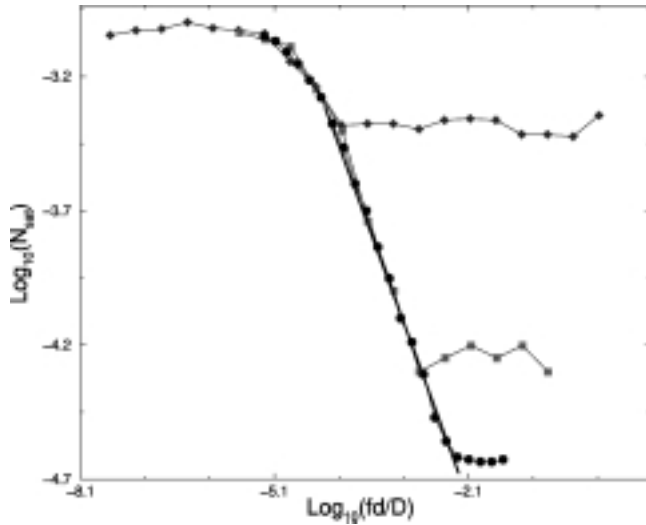


FIG. 2. Computer simulation of the saturation island density (obtained for a coverage of 10%) as a function of the rescaled chopping frequency fd/D . The rescaled flux is $F_i/D = 10^{-7}$, and each curve corresponds to a different value of d : $d = 0.1$ (diamonds) (lattice size $L = 400$), $d = 0.001$ (squares) (lattice size $L = 400$), $d = 0.0001$ (circles) (lattice size $L = 1500$). The solid line is a fit of the curve and has a slope 0.70 in excellent agreement with the predicted slope of $2/3$.

value of f ($f = 3 \times 10^{-5}$) is not due to a change of frequency as in the previous figure, but to the decrease of the flux which causes the decrease of the island density, and then the increase of the times $\tau_1 \approx 1/(D_1 N)$ and $\tau_2 \approx 1/(D_2 N)$.

In Fig. 4 we show the saturation island concentration as a function of the frequency for different values of i_{\max} . In each curve, the three regimes are present, and the bigger i_{\max} , the smaller the island density. This is easy to understand since small islands can aggregate with bigger islands, thus decreasing

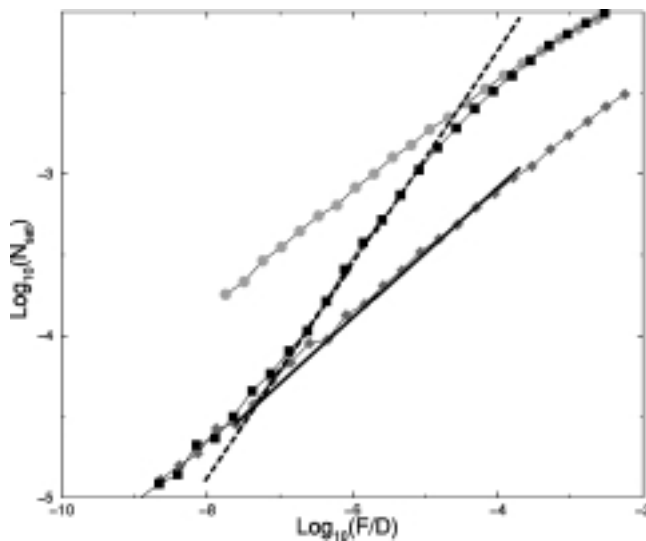


FIG. 3. Computer simulation of the saturation island density (obtained for a coverage of 10%) as a function of the rescaled flux F/D . The value of d is $d = 0.01$, the lattice size is $L = 400$ and each curve corresponds to a different value of the chopping frequency: $f = 10^{-1}$ (diamonds), 3×10^{-5} (squares), $f = 10^{-8}$ (circles). The dashed line has a slope $2/3$ and the solid line has a slope $2/5$.

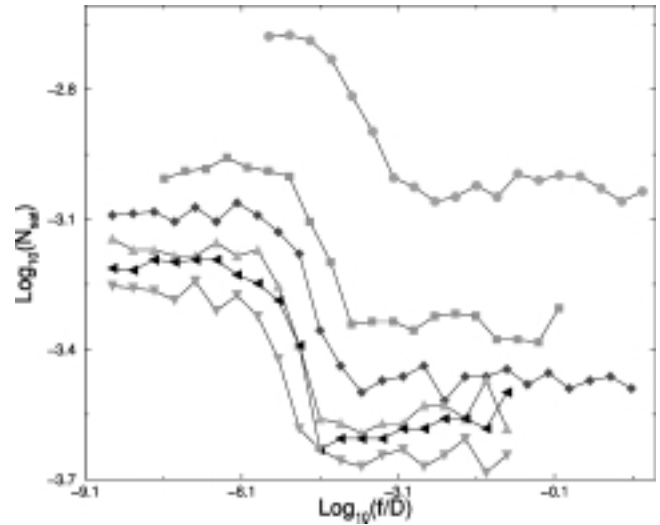


FIG. 4. Saturation island density (obtained for a coverage of 10%) as a function of the rescaled chopping frequency f/D . The rescaled flux is 10^{-7} , the value of d , 0.1, the lattice size, $L = 400$ and each curve corresponds to a different value of i_{\max} : $i_{\max} = 1$ (circles), $i_{\max} = 2$ (squares), $i_{\max} = 3$ (diamonds), $i_{\max} = 4$ (triangles up), $i_{\max} = 5$ (triangles left), $i_{\max} = 7$ (triangles down).

ing the total island density. Moreover, the decrease of the saturation island density leads to an increase of the mean aggregation time between the mobile species and the islands ($\tau_i \sim 1/N_{\text{sat}}$ where τ_i is the characteristic time for the islands of i particles to disappear from the substrate by aggregation on islands), which explains qualitatively the fact that the transition happens earlier when i_{\max} is bigger (the transition frequency is inversely proportional to this aggregation time).

II. REVERSIBLE AGGREGATION

The irreversible aggregation limit does not allow particles to leave an island: this is only realistic when the activation energy for a particle to detach is higher than thermal energy $k_B T$.

We will now study a model in which particles are allowed to leave the islands. We will assume that each particle has a bonding energy E_s with the substrate; and a bonding energy E_n with each neighbor. We assume that when a particle moves from one site to another, the particle goes through a transition state (Fig. 5) that has an energy independent of the initial and final states, and which we take as the origin of energies. Therefore, the activation energy for a particle to leave a lattice site is $E_s + jE_n$, where j is the number of neighbors of the particle: we assume that only the initial number of neighbors is relevant. The probability for that particle to move is taken proportional to $e^{-(E_s + jE_n)/k_B T}$. This is a classical ‘‘bond counting’’ model^{22–24} as recently used by Ratsch *et al.*¹⁸ The detailed balance is verified since the ratio of probabilities satisfies

$$\frac{p_{1 \rightarrow 2}}{p_{2 \rightarrow 1}} = e^{-[(n_1 - n_2)E_n]/k_B T},$$

where $p_{1 \rightarrow 2}$ is the probability for going from a state 1 (having n_1 neighbors) to a state 2 (having n_2 neighbors) and $p_{2 \rightarrow 1}$ is the probability for going from state 2 to state 1.

In the next section we will predict the behavior of the saturation island concentration for this model, including the presence of a chopped flux.

A. Scaling laws

To be able to perform simple calculations, we assume that only dimers can split to give two monomers, while all the bigger islands are stable. This simplification will be shown to lead to rather good predictions. We can give two plausible reasons to explain this: first, most particles belonging to large islands are multiply connected and will therefore not leave the island as easily as particles in dimers (which have only one neighbor) and second, the number of monomers (which our simplification underestimates since we neglect large island breaking) is in great part determined by the incident flux that is not affected by our simplified treatment.

The equations of the system then become

$$\frac{d\rho_1}{dt} \simeq F(t) - D_1\rho_1N + \frac{\rho_2}{\tau_b} - D_1\rho_1^2 - D_1\rho_1\rho_2, \quad (12)$$

$$\frac{d\rho_2}{dt} \simeq D_1\rho_1^2 - \frac{\rho_2}{\tau_b} - D_1\rho_1\rho_2. \quad (13)$$

These equations are almost the same as the ones obtained for the irreversible limit, but we have added to Eq. (12) a term of creation of monomers by disaggregation of dimers in a characteristic time τ_b (rigorously we should have put $2\rho_2/\tau_b$, but as we are only interested by scaling laws, we drop all geometrical factors); τ_b is related to the probability of breaking a single bond and therefore is proportional to $e^{-(E_n/kT)}$. Also, we have ignored certain process such as the motion of dimer due to shearing: we expect that such a process does not affect the exponent of the scaling laws.

Making the assumptions that $\rho_2 \ll \rho_1 \ll N$ and $\tau_b \ll 1/F$, which seems physically plausible if the incident flux is low enough, we obtain the simplified equations

$$\frac{d\rho_1}{dt} \simeq F(t) - \frac{\rho_1}{\tau_1}, \quad (14)$$

$$\frac{d\rho_2}{dt} \simeq D_1\rho_1^2 - \frac{\rho_2}{\tau_b}. \quad (15)$$

To solve these equations, we must take into account the five time scales $d/f, 1/f, \tau_1, \tau_b, \tau_N$, where τ_N is the charac-

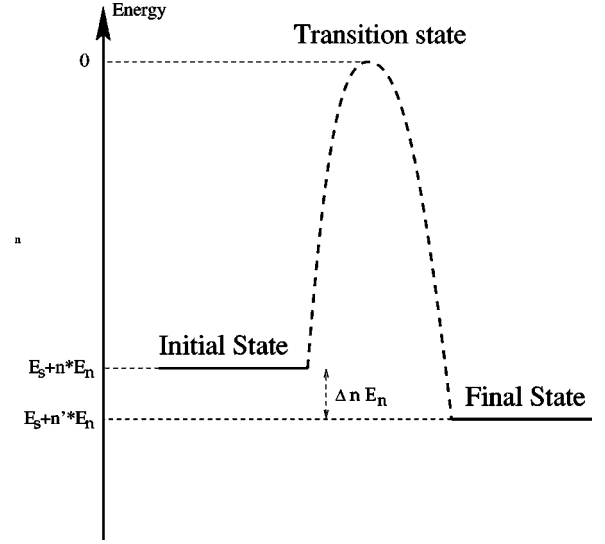


FIG. 5. Illustration of the energy landscape as seen by a diffusing particle. The energy barrier for a given jump depends only on the initial number of bonds (n). This automatically satisfies the detailed balance (see text).

teristic time of evolution of the islands concentration (since the typical time needed to reach saturation is a fraction of a monolayer, an estimate of this time is $\tau_N \simeq N/F_i$; see also the preceding section). We will assume that τ_N is bigger than all other time scales. Let's study what happens as a function of d and f for the different values of τ_1 and τ_b .

In the case $\tau_1 \ll d/f$, the monomer concentration reaches its steady value almost instantaneously:

$$0 < t < d/f, \quad \rho_1(t) = \frac{F_i}{D_1N}, \quad (16)$$

$$d/f < t < 1/f, \quad \rho_1(t) = 0. \quad (17)$$

And so we can solve Eq. (15):

$$0 < t < d/f, \quad \rho_2(t) = \tau_b D_1 \left(\frac{F_i}{D_1N} \right)^2 (1 - e^{-t/\tau_b}), \quad (18)$$

$$d/f < t < 1/f, \quad \rho_2(t) = \tau_b D_1 \left(\frac{F_i}{D_1N} \right)^2 (1 - e^{-d/f\tau_b}) e^{-t/\tau_b}. \quad (19)$$

TABLE I. Scaling law for the different regimes.

	$\tau_b \ll d/f$	$d/f \ll \tau_b \ll 1/f$	$1/f \ll \tau_b$
		$\tau_b \ll \tau_1 \tau_1 \ll \tau_b$	
$\tau_1 \ll d/f$	$\left(\frac{\tau_b}{D_1} \right)^{1/4} F_i^{1/2}$	$\left(\frac{d}{D_1 f} \right)^{1/4} F_i^{1/2}$	$\left(\frac{\tau_b}{D_1} \right)^{1/4} d^{1/4} F_i^{1/2}$
$d/f \ll \tau_1 \ll 1/f$	$(\tau_b D_1)^{1/2} \frac{F_i d}{f}$	$(\tau_b D_1)^{1/2} \frac{F_i d}{f} \left(\frac{F_i d}{f} \right)^{2/3}$	$\left(\frac{F_i d}{f} \right)^{2/3} (\tau_b f)^{1/3}$
$1/f \ll \tau_1$	$\left(\frac{\tau_b}{D_1} \right)^{1/4} (F_i d)^{1/2}$	$\left(\frac{\tau_b}{D_1} \right)^{1/4} (F_i d)^{1/2}$	$\left(\frac{\tau_b}{D_1} \right)^{1/4} (F_i d)^{1/2}$

Since N increases each cycle by $\Delta N_{\text{cycle}} = \int D_1 \rho_1 \rho_2 dt$, we obtain the following scaling laws [the number of cycles is a function of the coverage θ : $n_{\text{cycle}} = \theta f / F_i d$, see the preceding section]: if $\tau_b \ll d/f$ then

$$N_{\text{sat}} \sim \left(\frac{\tau_b}{D_1} \right)^{1/4} F_i^{1/2}, \quad (20)$$

if $d/f \ll \tau_b \ll 1/f$ then

$$N_{\text{sat}} \sim \left(\frac{d}{D_1 f} \right)^{1/4} F_i^{1/2}. \quad (21)$$

If $1/f \ll \tau_b$ then the dimer concentration has not enough time to vanish at the end of the period. It reaches an almost constant value during the period: $\rho_2 = d \tau_b D_1 (F_i / D_1 N)^2$. The saturation island concentration becomes

$$N_{\text{sat}} \sim \left(\frac{\tau_b}{D_1} \right)^{1/4} d^{1/4} F_i^{1/2}. \quad (22)$$

We can check that these three results are compatible each other: for instance, if $\tau_b \rightarrow d/f$, Eq. (20) gives Eq. (21) changing τ_b by d/f .

In the case $d/f \ll \tau_1 \ll 1/f$, we have to solve exactly Eqs. (14) and (15) and we finally obtain the following: if $\tau_b \ll d/f$ then

$$N_{\text{sat}} \sim \left(\frac{F_i d}{f} \right)^{2/3} (\tau_b f)^{1/3}, \quad (23)$$

if $d/f \ll \tau_b \ll 1/f$ then

$$\tau_1 \ll \tau_b, \quad N_{\text{sat}} \sim \left(\frac{F_i d}{f} \right)^{2/3}, \quad (24)$$

$$\tau_b \ll \tau_1 N_{\text{sat}} \sim (D_1 \tau_b)^{1/2} \frac{F_i d}{f}; \quad (25)$$

if $1/f \ll \tau_b$ then

$$N_{\text{sat}} \sim \left(\frac{F_i d}{f} \right)^{2/3} (\tau_b f)^{1/3}. \quad (26)$$

In the case $1/f \ll \tau_1$, the monomer concentration is almost constant during each period and, since the dimer concentration is entirely controlled by the monomer one, the dimer concentration is also almost constant, and then we obtain the same scaling law for all the cases $\tau_b \ll d/f, d/f \ll \tau_b \ll 1/f$ and $1/f \ll \tau_b$:

$$N_{\text{sat}} \sim \left(\frac{\tau_b}{D_1} \right)^{1/4} (F_i d)^{1/2}. \quad (27)$$

This relation is similar to Eq. (28) of Ref. 10

We let the reader check the compatibility of all these results, which we have summarized in Table I.

This table present all the regimes found, but some of them are not very physical or unreachable by simulations. For instance, the case $1/f \ll \tau_1$ and $\tau_b \ll d/f$ would represent a system where particles would leave islands very quickly, and it would take a very long time to obtain some large islands; and, moreover, simulations in this case would be very expen-

sive in computer time. On the other hand, in our predictions we made the assumption that $\tau_1, \tau_b \ll \tau_N$, and we must take care to stay with in these hypothesis in simulations: one could show that the case $\tau_1 \ll d/f$ and $1/f \ll \tau_b$ is very hard to reach by simulations, and we will not see it.

Finally, one can be surprised because in the case $\tau_b \rightarrow +\infty$, we do not find the same results as in irreversible aggregation;¹⁴ in fact, our assumption $\tau_b \ll \tau_N$ forbids $\tau_b \rightarrow +\infty$.

B. Computer simulation

As in the irreversible limit, we use a Monte Carlo simulation, and we take into account only two processes: (i) *Deposition*. Particles are dropped on the substrate with a flux F_i when the flux is on, and no particle is dropped when the flux is off. (ii) *Diffusion*. Particles diffuse with a probability that depends on the number of neighbors. More precisely, the

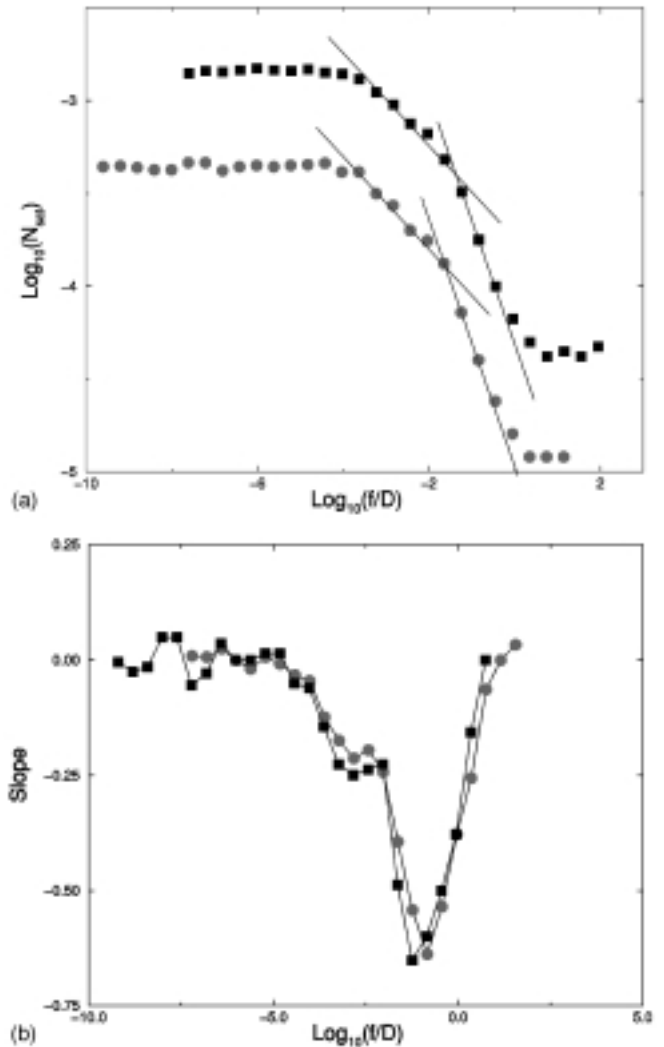


FIG. 6. Saturation island density (obtained for a coverage of 10%) as a function of the rescaled frequency (a) and the corresponding slope (b). The value of d is 0.001, the lattice size is $L = 600$ and each curves correspond to different values of energies and flux: $E_s = 1.3, E_n = 0.5, F_{i/D} = 10^{-7}$ (squares), $E_s = 1.42, E_n = 0.4, F_{i/D} = 6 \times 10^{-7}$ (circles). The solid lines have slopes $-1/4$ and $-2/3$.

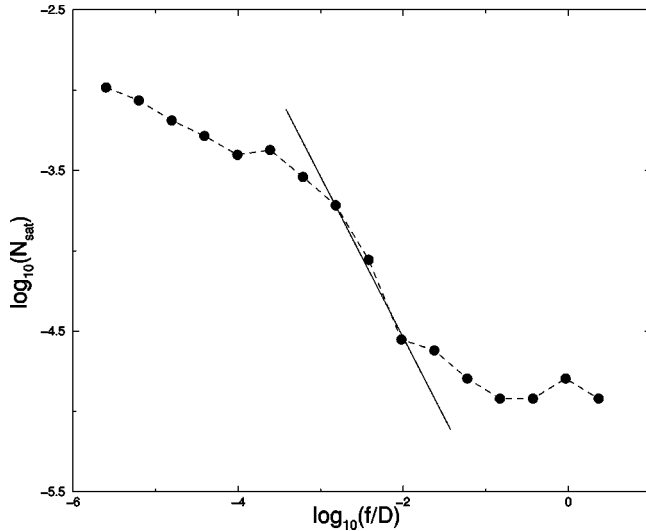


FIG. 7. Saturation island density (obtained for a coverage of 10%) as a function of the rescaled frequency. The rescaled flux (F/D) is 10^{-7} , d is 0.001, the lattice size is $L=500$ and values of energy are $E_s=1.3$, $E_n=0.4$. The solid line has a slope -1 .

probability for a particle with j neighbors to move is taken proportional to $e^{-(E_s+jE_n)/k_B T}$.

To ensure this, the algorithm is written to have, for each loop, a probability of depositing a new particle:

$$P_{\text{drop}} = \frac{F_i L^2 \tau}{F_i L^2 \tau + \sum_i \frac{(6-i)}{6} n_i e^{-iE_n/k_B T}} \quad (28)$$

and the probability to move a particle with i_0 neighbors:²⁴

$$P_{i_0} = \frac{\frac{(6-i_0)}{6} n_{i_0} e^{-i_0 E_n/k_B T}}{F_i L^2 \tau + \sum_i \frac{(6-i)}{6} n_i e^{-iE_n/k_B T}}, \quad (29)$$

where $\tau = \nu_0^{-1} e^{E_s/k_B T}$ (Refs. 18,24) is the diffusion time for a particle without neighbors, ν_0 is a typical vibration frequency ($\nu_0 = 10^{13} \text{ s}^{-1}$), n_i is the number of particles with

i neighbors (we only allow to particles with less than four neighbors to move), k_B is the Boltzmann constant, T is the temperature, L is the lattice linear size, and the factors $(6-i)$ serve to accelerate the algorithm.²⁵

As for the irreversible aggregation, we studied the saturation island density dependence on the chopping frequency. Figure 6 shows the results obtained for values of E_n and E_s such that $\tau_1 \leq \tau_b$ and $\tau_1/\tau_b \ll d$. We can first check that the ratio between the island density in the low- and high-frequency regimes corresponds to $d^{1/2}$. According to Table I, by increasing the frequency we should scan successively the regimes of slopes 0, $-1/4$, $-2/3$ (or -1 , since τ_1 and τ_b are very close) and finally 0. We can check in Fig. 6 that the slope of the curve takes successively the values 0, $-1/4$, ~ -0.64 and 0, in good agreement with the prediction.

Figure 7 shows the results obtained for values of E_n and E_s such that $\tau_b \leq \tau_1$. Here, increasing the frequency should lead to successive slopes of 0, -1 , 0. Figure 7 shows that the three regimes are present.

In conclusion, these two figures confirm the theoretical predictions with good accuracy taking into account the approximations we have done to obtain Table I.

III. CONCLUSION

In this work, we have studied the influence of a chopped flux in two models of deposition of atoms on a surface: a model of irreversible aggregation with mobile islands, and a model of reversible aggregation more adapted for high temperatures.

Mean-field-like equations have allowed us to calculate the different scaling laws verified by the saturation island density as a function of the different parameters of the growth. Several regimes were obtained as a function of the chopping frequency. These results were checked by Monte Carlo simulations, leading to a very good agreement.

These results are useful for films grown with intrinsically pulsed beams¹³ as well as for investigating new growth regimes with continuous sources equipped with a chopper. It should be noted that chopping the flux permits to act on the kinetics of the growth just as temperature does but with a much more specific action, since temperature acts on all activated processes.

* Author to whom correspondence should be addressed. Electronic address: jensen@dpm.univ-lyon1.fr

¹G. Zinsmeister, *Vacuum* **16**, 529 (1966); *Thin Solid Films* **2**, 497 (1968); **4**, 363 (1969); **7**, 51 (1971).

²Y.W. Mo, J. Kleiner, M.B. Webb, and M.G. Lagally, *Phys. Rev. Lett.* **66**, 1998 (1991).

³H. Brune, H. Röder, C. Borragno, and K. Kern, *Phys. Rev. Lett.* **73**, 1955 (1994).

⁴J.A. Strosio and D.T. Pierce, *J. Vac. Sci. Technol. B* **12**, 1783 (1994).

⁵L.-H. Tang, *J. Phys. I* **3**, 935 (1993); J.W. Evans and M.C. Bartelt, *J. Phys. I* **12**, 1800 (1994); G.S. Bales and D.C. Chrzan, *Phys. Rev. B* **50**, 6057 (1994). For a review, see A.-L. Barabasi and H.E. Stanley, *Fractal Concepts in Surface Growth* (Cambridge University Press, 1995); J. Villain and A. Pimpinelli *Physique de la Croissance Cristalline* (Eyrolles, Paris, 1995).

⁶P. Jensen, A.-L. Barabási, H. Larralde, S. Havlin, and H.E. Stan-

ley, *Nature (London)* **368**, 22 (1994); *Phys. Rev. B* **50**, 15 316 (1994).

⁷J.M. Wen, S.L. Chang, J.W. Burnett, J.W. Evans, and P.A. Thiel, *Phys. Rev. Lett.* **73**, 2591 (1994).

⁸P. Deltour, P. Jensen, and J.L. Barrat, *Phys. Rev. Lett.* **78**, 4597 (1997).

⁹M. Lagally, *Phys. Today* **46** (11), 24 (1993) and references therein.

¹⁰J. Villain, A. Pimpinelli, L.-H. Tang, and D.E. Wolf, *J. Phys. I* **2**, 2107 (1992).

¹¹J.A. Venables, G.D.T. Spiller, and M. Hanbücken, *Rep. Prog. Phys.* **47**, 399 (1984).

¹²S. Stoyanov and D. Kaschiev, *Current Topics in Materials Science*, edited by E. Kaldis (North-Holland, Amsterdam, 1981), Vol. 7.

¹³P. Melinon, V. Paillard, V. Dupuis, A. Perez, P. Jensen, A. Hoareau, J.P. Perez, J. Tuillon, M. Broyer, J.L. Vialle, M. Pellarin,

- B. Baguenard, and J. Lerme, *J. Phys. I* **3**, 1585 (1993); A. Perez, P. Melinon, V. Dupuis, P. Jensen, B. Prevel, J. Tuaille, L. Bardotti, C. Martet, M. Treilleux, M. Broyer, M. Pellarin, J.I. Vialle, and B. Palpant, *J. Phys. D* **30**, 1 (1997).
- ¹⁴P. Jensen and B. Niemeyer, *Surf. Sci. Lett.* **384**, 823 (1997).
- ¹⁵S. Liu, L. Bönig, and H. Metiu, *Phys. Rev. B* **52**, 2907 (1995).
- ¹⁶L. Bardotti, P. Jensen, A. Hoareau, M. Treilleux, B. Cabaud, A. Perez, F. Cadete, and Santos Aires, *Surf. Sci.* **367**, 276 (1996).
- ¹⁷M.C. Bartelt, S. Gunther, E. Kopatzi, R.J. Behm, and J.W. Evans, *Phys. Rev. B* **53**, 4099 (1996).
- ¹⁸C. Ratsch, P. Smilauer, A. Zangwill, and D.D. Vvendsky, *Surf. Sci.* **329**, L599 (1995).
- ¹⁹M.C. Bartelt and J.W. Evans, *Phys. Rev. B* **46**, 12 675 (1992).
- ²⁰P. Jensen, H. Larralde, and A. Pimpinelli, *Phys. Rev. B* **55**, 2556 (1997).
- ²¹J.A. Venables, *Philos. Mag.* **27**, 697 (1973).
- ²²S. Clarke and D.D. Vvendsky, *Phys. Rev. Lett.* **58**, 2235 (1987).
- ²³M. Schroeder, P. Smilauer, and D.E. Wolf, *Phys. Rev. B* **55**, 10 814 (1997).
- ²⁴H.C. Kang and W.H. Weinberg, *J. Chem. Phys.* **90**, 2824 (1989).
- ²⁵Y.T. Lu and H. Metiu, *Surf. Sci.* **245**, 150 (1991).